SCIENTIFIC REPORTS

OPEN

Different adsorption-degradation behavior of methylene blue and Congo red in nanoceria/H_2O_2 system under alkaline conditions

Received: 1 March 2018
Accepted: 22 November 2018
Published online: 21 March 2019

Xiaoshu Wei, Yi Wang, Yuqian Feng, Xiaomin Xie, Xiaofeng Li & Sen Yang

The Fenton-like activity of nanoceria has attracted intensive attention for wastewater treatment in recent years. During the Fenton-like reaction, the adsorption of organic pollutants on catalyst surface plays a key role in their degradation. In this work, the adsorption-degradation of methylene blue (MB) and Congo red (CR) in nanoceria/H_2O_2 system was investigated under alkaline conditions. The MB exhibited weak adsorption on nanoceria surface via electrostatic attraction, while strong Lewis acid–base interactions between CR and cerium ions was observed. Moreover, the adsorption of MB was enhanced in the presence of H_2O_2 by the formation of surface peroxide species, but an adsorption competition existed between H_2O_2 and CR. With more Ce^{3+}, CeO_2 nanorods could degrade CR efficiently as Fenton-like catalyst. But the degradation of MB catalyzed by ceria was much lower than that of CR in the presence of H_2O_2.

Recently, many studies have suggested that ceria nanoparticles (nanoceria) can act as a Fenton-like catalyst, based on observations of the oxidation reaction of organic compounds in the presence of H_2O_2[1–3]. The Fenton-like activity of nanoceria has been ascribed to some active oxidative species that can be generated during the catalytic decomposition of H_2O_2[4–6]. In 2008, Heckert *et al.*[4] first reported that a cerous salt solution could catalyze the decomposition of H_2O_2 and generate HO· through a Fenton-like reaction. Later, the formation of HO· was confirmed in nanoceria/H_2O_2 system[7]. On the other hand, Chen and co-workers[8–10] revealed that H_2O_2 could react with cerium ions on the surface of nanoceria and form stable brown peroxide species, which would induce an intermolecular rearrangement with the adjacent adsorbed organic compounds to achieve the degradation of organics or generate HO· through a homolytic cleavage of the O–O bond to attack the neighboring adsorbed organics[5]. Now, it is recognized that the catalytic activity of nanoceria relies closely on the redox cycle between Ce^{3+} and Ce^{4+}, and a higher level of Ce^{3+} and defects can generate more active oxidative species and exhibit better activity toward the oxidative degradation of organic compounds[11,12].

The oxidation reaction of organic compounds in nanoceria/H_2O_2 system generally occurs on the ceria surface; therefore, the adsorption of organics plays an important role in their degradation[10,13]. Previous studies have shown that nanoceria exhibits high degradation activity for the adsorbable organic compounds such as orange II, methyl orange, salicylic acid[8,14]; however, the degradation of weakly adsorbed organic compounds such as rhodamine B, rhodamine 6 G and catechol hardly occurs[6,8]. Actually, the adsorption of organics depends on the structures of organic compounds, the surface chemistry of adsorbent and the solution conditions[15,16]. According to adsorbate–adsorbent interactions, the adsorption can be classified as chemical adsorption and physical adsorption[16]. Chemical adsorption means the formation of strong chemical associations between adsorbate and adsorbent; therefore, chemical adsorption is usually irreversible. Physical adsorption is reversible and the main physical forces controlling adsorption are van der Waals forces, hydrogen bonds and polarity[17]. The presence of H_2O_2 also influences the adsorption of organic compounds over nanoceria surface. For example, the adsorption competition between H_2O_2 and orange II has been observed[5,13], and the degradation of orange II was inhibited by over-complexation of H_2O_2 with CeO_2[10,18]. Because of the importance of adsorption in Fenton-like processes, it

Beijing Key Laboratory of Farmland Soil Pollution Prevention and Remediation, College of Resources and Environmental Sciences, China Agricultural University, Beijing, 100193, China. Correspondence and requests for materials should be addressed to S.Y. (email: syang@cau.edu.cn)

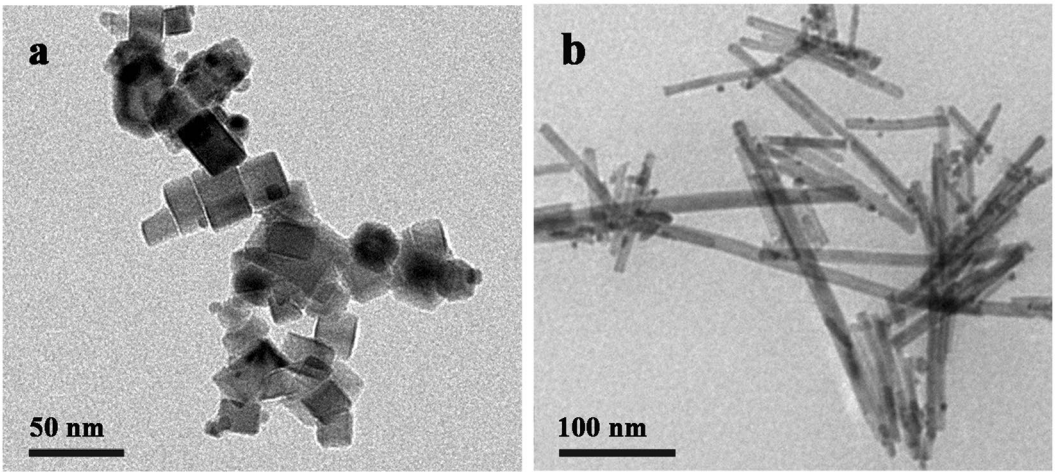

Figure 1. TEM images of CeO_2 nanocubes (**a**) and nanorods (**b**).

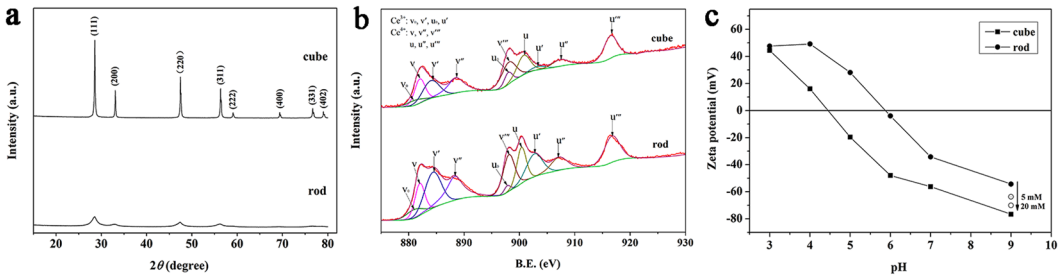

Figure 2. XRD patterns (**a**), Ce3d XPS spectra (**b**) and the zeta potential as a function of pH of CeO_2 nanorods and nanocubes (**c**).

is highly desirable to investigate the adsorption behavior of organic compounds in nanoceria/H_2O_2 system and their effect on the degradation of organic compounds.

Today, more than 100,000 commercial dyes with different chemical structures are widely used for printing and dyeing and a portion is discharged with wastewater[19,20]. Several methods such as advanced oxidation and adsorption are used to decolorize dye wastewater[16,21]. Fenton-like reaction is found to be efficient for the removal of organic pollutants from wastewater[21–23]. Generally, pH has an important effect on the efficiency of Fenton-like catalysts such as Cu-based bimetallic oxides, Fe_3O_4@cellulose aerogel nanocomposite and Mn-doped $BiFeO_3$ nanoparticles[24–26]. Some studies showed that the optimum working condition is acidic condition, while others reported that some catalysts could efficiently decompose H_2O_2 even at near-neutral or neutral conditions[27,28]. These researches mainly focus on the acidic and neutral pH conditions. As we know, Aneggi *et al.*[2] firstly reported that ceria and ceria-zirconia solid solutions could be effectively used for the treatment of landfill leachate at pH 9.0. Actually, the wastewater generated during printing and dyeing is characterized by a high pH value[29]. Then, methylene blue (MB), one of the major thiazine dyes, was chosen as a representative for cationic dyes, and Congo red (CR), one of the major azo dyes was used as a model for anionic dyes. CeO_2 nanocubes and nanorods were prepared by a hydrothermal method and were used as Fenton-like catalysts for the degradation of dyes in the presence of H_2O_2. The adsorption of dyes on ceria surface in the presence or absence of H_2O_2 was investigated to better understand their degradation in nanoceria/H_2O_2 system under alkaline conditions.

Results and Discussion

Characterization of nanoceria. Nanoceria was synthesized through a hydrothermal process. The morphologies and sizes of nanoceria were studied by transmission electron microscopy (TEM). As in our previous study[30,31], the CeO_2 nanocubes had uniform cubic shapes with a size of 20–30 nm (Fig. 1a), while the CeO_2 nanorods had diameters of approximately 15–20 nm and lengths of 100–200 nm (Fig. 1b). Dynamic light scattering analysis was performed to detect the agglomeration size of nanoceria in pH 9.0 of aqueous solution. As shown in Fig. S1, both of nanocubes and nanorods are inclined to agglomerate into larger particles with similar size.

The phase purity and crystal structure of CeO_2 nanocubes and nanorods were identified by XRD (Fig. 2a). All the diffraction peaks of both samples can be indexed to the pure fluorite structure of CeO_2 (JCPDS 34–0394). Meanwhile, the nanocubes exhibited sharper XRD diffraction peaks than those of the nanorods, indicating a higher crystallinity and bigger crystallite size of the nanocubes[32]. The surface chemistry of nanoceria was analyzed by XPS. The XPS survey scan is given in Fig. S2. The possibility of appearance of sodium on the surface of nanoceria can be ruled out because no peaks belonging to sodium were detected. The Ce(*3d*) XPS spectra are

shown in Fig. 2b. Peak v_o, v', u_o and u' belong to Ce^{3+} species, while v, v'', v''', u, u'' and u''' are derived from Ce^{4+}. The relative concentration of Ce^{3+} on the surface of nanoceria was calculated as follows[33]:

$$[Ce^{3+}] = \frac{A_{v0} + A_{v'} + A_{u0} + A_{u'}}{A_{v0} + A_{v'} + A_{u0} + A_{u'} + A_{v} + A_{v''} + A_{v'''} + A_{u} + A_{u''} + A_{u'''}} \times 100\% \quad (1)$$

where A_i is the integrated area of peak 'i'.

The relative concentration of Ce^{3+} on the surface of nanorods was 42.9%, which was much larger than that of nanocubes (36.5%). The O(*1 s*) spectra for both samples are shown in Fig. S3. The peak with a binding energy of around 529 eV can be ascribed to the lattice oxygen species of bulk CeO_2 (O_{lat}); the peak with a binding energy of around 531 eV is attributed to surface chemisorbed oxygen (O_{sur}) and the peak at around 533 eV is assigned to molecular water adsorbed on the surface[34–36]. According to the literature[34–36], the relative concentration of O_{sur} is estimated from the relative areas of peaks. The ratios of $O_{sur}/(O_{lat} + O_{sur})$ are approximately 50.6% and 59.4% for nanocubes and nanorods, respectively. The higher proportion of chemisorbed oxygen in nanorods may due to their higher Ce^{3+} concentration. Because Ce^{3+} in nanoceria can generate oxygen vacancies and then facilitate oxygen adsorption[37].

The zeta potential of nanoceria was determined as a function of pH, and the isoelectric points (PI) of nanocubes and nanorods was at approximately pH 4.5 and 5.8, respectively (Fig. 2c). The specific surface areas of nanoceria were measured by nitrogen gas adsorption/desorption isotherm and calculated by BET method. The nanorods exhibit a larger surface area (89.9 $m^2 g^{-1}$) than that of nanocubes (39.7 $m^2 g^{-1}$).

Adsorption of MB and CR on nanoceria in the absence of H_2O_2. To understand the decolorization of MB and CR in nanoceria/H_2O_2 system, the adsorption of dyes on nanoceria surface was surveyed in the absence of H_2O_2 at first, and the adsorbed amount of dye was determined after 30 min of equilibrium time. The amount of MB adsorbed on CeO_2 nanorods and nanocubes was only 0.01 mg m^{-2} and 0.11 mg m^{-2}, respectively. The results showed that the adsorption of MB on CeO_2 surface was very weak. Interestingly, a large amount of negatively charged CR was adsorbed: 0.78 mg m^{-2} on the nanorods surface and 0.39 mg m^{-2} on the nanocubes surface (Fig. S4a).

The different adsorption behavior could be possibly explained by the different structures of MB and CR. At pH 9.0, nanocubes and nanorods are negatively charged (Fig. 2c), and MB is positively charged. Under these conditions, MB adsorption on the nanoceria surface mainly takes place through electrostatic attraction, and the higher adsorption capacity of nanocubes may be owing to the higher negative charge[38]. Similar adsorption behavior has also been observed for cationic dye rhodamine B (RhB) and Orange II, which were adsorbed by CeO_2 through strong electrostatic attraction[13,39]. However, the electrostatic repulsion between CR and nanoceria means that the strong adsorption of CR was not based on the electrostatic interaction. *Ex situ* FT-IR data indicated that acid orange 7 (AO7), an azo dye, could be adsorbed on nanoceria surface via a Lewis acid–base reaction between cerium ions and the oxygen atoms of sulfonate group of azo dye[40]. Srilakshmi[41] reported that Ag-modified calcium hydroxyapatite (CaHAp) exhibited high adsorption capacity for CR adsorption because of its high Lewis acidity. Thus, we speculated that CR adsorption was based on the Lewis acid−base reaction, and more Ce^{3+} on nanoceria surface resulted in a higher adsorption capacity.

To further investigate the adsorption mechanism, desorption study was performed using HCl aqueous solution with pH of 3.0 as the eluting agent. For the desorption study, the dye-loaded nanoceria was isolated from pH 9.0 suspension and added into the HCl aqueous solution. A quick desorption of MB occurred. The colorless acid aqueous solution became blue almost immediately after the introduction of MB-loaded nanoceria. The occurrence of desorption could be explained by electrostatic repulsion between MB and nanoceria because the surface of nanoceria is positively charged at pH 3.0. Therefore, we can conclude that both nanocubes and nanorods could adsorb MB through electrostatic adsorption when the pH of solution was higher than their PI and the adsorption of MB was reversible. However, the desorption of CR did not occur and the adsorbed CR retained its red color in the HCl aqueous solution, even though free CR is a pH indicator and should turn blue at pH 3.0. The strong adsorption of CR on nanoceria further indicated that the interaction between CR and ceria surface could be owing to the strong Lewis acid–base interactions.

Decomposition of H_2O_2 over CeO_2. The catalytic H_2O_2 decomposition over CeO_2 nanorods and nanocubes was investigated at 25 °C. As shown in Fig. 3, 82.7% of 20 mM H_2O_2 was decomposed after 120 min in the presence of nanorods, while only 38.8% in the presence of nanocubes under the same conditions. Generally, the catalytic activity of nanoceria is directly related to its surface chemical states and specific surface area[11]. The high concentration of Ce^{3+} facilitates the adsorption and decomposition of H_2O_2[4,5,42]. Hence, the high activity of nanorods was owing to the presence of more Ce^{3+}, as proved by XPS analysis.

To probe the oxidative species during the catalytic decomposition of H_2O_2 over nanoceria, EPR spectroscopy measurement was performed using DMPO as a spin trap. As shown in Fig. S5, a typical signal of DMPO-OH adducts (1:2:2:1 quartet) was detected for a suspension of nanorods upon the addition of H_2O_2, which suggested the generation of HO· in the catalytic decomposition of H_2O_2. Similar results were obtained for a suspension of nanocubes, except the low intensity of the DMPO-OH peaks. Fig. S6 showed the Raman spectra of CeO_2 nanorods before and after H_2O_2 treatment at pH 9.0. The appearance of band at 830 cm^{-1} indicates the presence of the η^2-peroxide (O_2^{2-}) species on the surface of CeO_2 nanorods after H_2O_2 treatment[8,43,44]. These results suggest that the presence of HO· and peroxide-like intermediates in nanoceria/H_2O_2 system at pH 9.0. Hamoud *et al.*[13] suggested the relationship between surface Ce(IV) peroxo species and HO· radicals production:

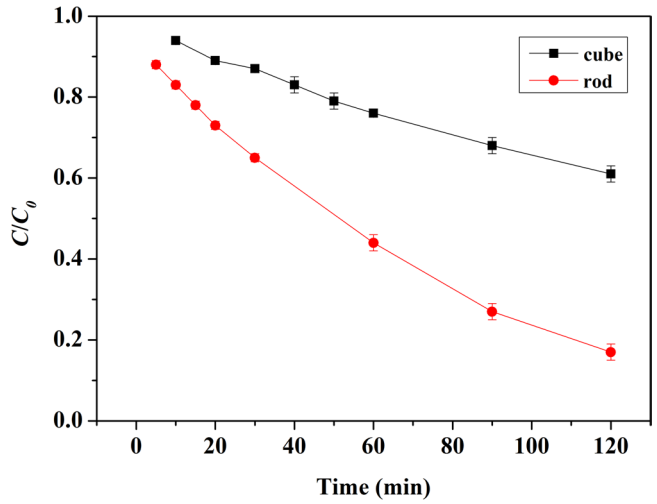

Figure 3. H_2O_2 decomposition over CeO_2 nanorods and nanocubes (1.0 g L^{-1} CeO_2, 20 mM H_2O_2, 25 °C).

$$Ce^{3+} + \frac{3}{2}H_2O_2 \rightarrow Ce^{4+}(O_2)^{2-} + H_2O + H^+ \quad (2)$$

$$Ce^{4+}(O_2)^{2-} + 2H^+ \rightarrow Ce^{4+} + 2HO\cdot \quad (3)$$

Decolorization of MB in nanoceria/H_2O_2 system. *Effect of H_2O_2 concentration on decolorization of MB.* Pre-experiments showed that little change in MB concentration was observed with H_2O_2, however, upon introduction of H_2O_2 into suspension of nanoceria with MB, the color of nanocubes and nanorods became deep blue and green in 5–10 min, respectively (Fig. S7). Obviously, the adsorption of MB on nanoceria was enhanced in the presence of H_2O_2. And the decolorization of MB in nanoceria/H_2O_2 system can be ascribed to both adsorption and oxidative degradation. Then the total amount of MB (labeled as MB_t) in suspension was divided into three parts: (1) free MB (labeled as MB_f) in supernatant; (2) adsorbed MB (labeled as MB_a) on nanoceria surface; and (3) degraded MB (labeled as MB_d) in nanoceria/H_2O_2 system, which was determined by the difference in the amount of MB_t, MB_f and MB_a:

$$MB_d = MB_t - MB_f - MB_a \quad (4)$$

When the concentration of H_2O_2 was 20 mM, the decolorization of MB after 30 min in both nanoceria/H_2O_2 systems was investigated. In the case of nanorods, 80.3% of MB was decolorized; in the case of nanocubes, the decolorization was 76.2% (Fig. 4). However, when the nanoceria was isolated from both systems and added into pH 3.0 HCl aqueous solution, desorption occurred and the amount of desorbed MB was almost equal to the amount of decolorization. The results clearly suggested that the decolorization of MB in nanoceria/H_2O_2 system was mainly due to adsorption rather than degradation at 30 min. Meanwhile, the enhanced adsorption of MB on nanoceria surface caused by the presence of H_2O_2 was reversible and could be totally desorbed using pH 3.0 HCl aqueous solution as the eluting agent.

The influence of H_2O_2 concentration on MB adsorption on nanoceria surface was further investigated. The contact time was limited to 30 min to avoid the interference of degradation of MB. As shown in Fig. 5, upon the introduction of 5 mM H_2O_2, the adsorbed amount of MB on CeO_2 nanorods and nanocubes increased by 6.6 and 1.3 times in 30 min, respectively. In the case of nanorods, the adsorbed amount of MB increased with increasing H_2O_2 concentration from 5 mM to 20 mM and then remained almost unchanged. However, further increase of the H_2O_2 concentration did not have a significant influence on the adsorption of MB in the presence of nanocubes.

The effect of H_2O_2 on the zeta potential of nanoceria at pH 9.0 was investigated. It is clear that the addition of H_2O_2 made the zeta potential of CeO_2 nanorods more negative, and the absolute value of the zeta potential increased from 5 mM to 20 mM of H_2O_2 (Fig. 2c). However, the zeta-potential of CeO_2 nanocubes did not change obviously in the presence of H_2O_2 (data not show). The increased negative zeta-potential of CeO_2 nanorods may be attributed to the formation of negative surface peroxide species via Ce^{3+}–H_2O_2 interactions[43,45]. The generation of surface peroxide species increased with increasing H_2O_2 concentration until the Ce^{3+} sites of nanoceria surface were completely occupied[5,13]. The unchanged zeta-potential of CeO_2 nanocubes may be explained by the presence of less Ce^{3+} sites and higher original zeta-potential. Because the adsorption of MB on nanoceria surface is via electrostatic adsorption, we speculate that the negatively charged surface peroxide species on the surface of nanoceria may be an important reason for the enhanced adsorption of MB on nanoceria, especially on the nanorods.

Effect of contact time on MB decolorization. To further investigate the catalytic oxidation of MB in nanoceria/H_2O_2 system, the effect of contact time on the decolorization of MB was investigated. Figure 6a shows the UV–vis

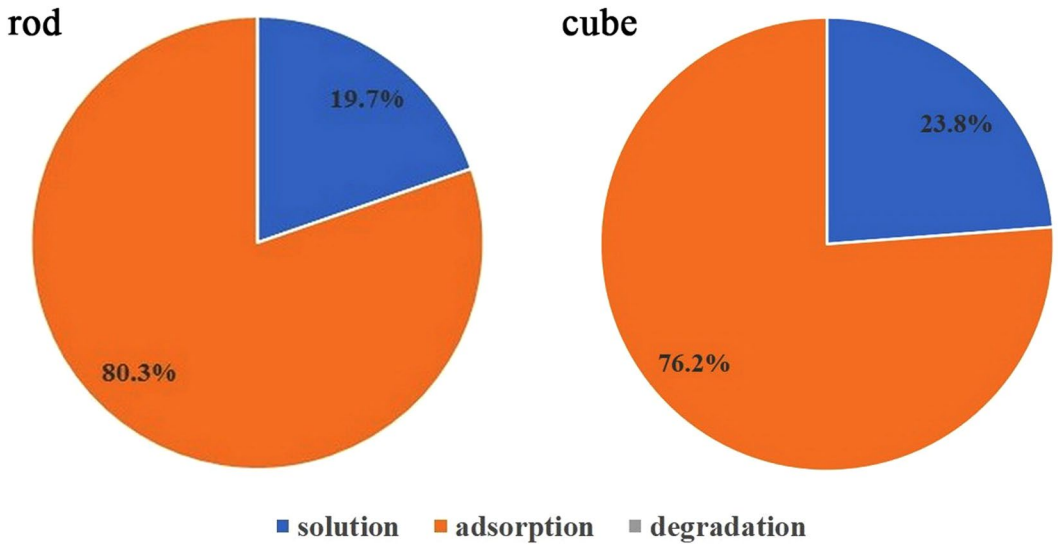

Figure 4. Distribution of MB in nanoceria/H_2O_2 system at 30 min.

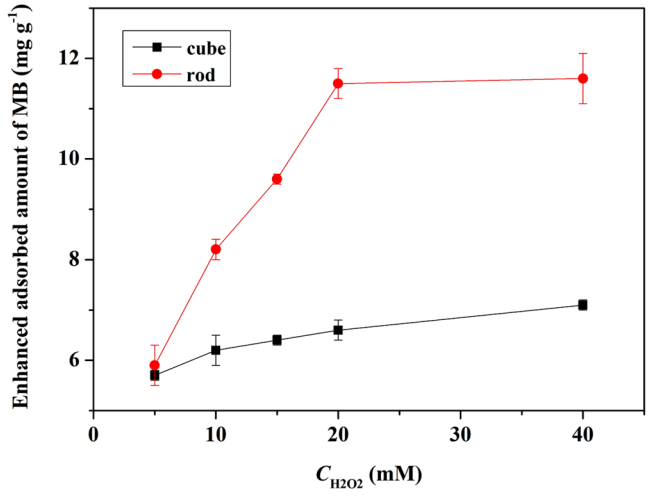

Figure 5. The effect of H_2O_2 concentration on the adsorption of MB on nanoceria surface (15 mg L^{-1} MB, 1.0 g L^{-1} CeO_2, 25 °C, pH 9.0).

spectral changes of the supernatant as a function of time. Upon the addition of H_2O_2 to the suspension of nanorods/MB, the characteristic band (centered at 664 nm) of MB decreased immediately, after which it continued to decrease up to 30 min, and then began to increase up to 12 h. The UV–vis spectra showed that the concentration of MB in supernatant had a special change: it first decreased and then increased.

To understand the decolorization of MB in CeO_2 nanorods/H_2O_2 system, the distribution of MB in suspension at 12 h was analyzed and is shown in Fig. 7; most of MB was dissolved in supernatant, 15.8% was degraded and only 4.8% was adsorbed. These results indicated that MB could be degraded in suspension of nanocubes/H_2O_2 at pH 9.0, although the rate of degradation was rather slow. The special change of MB concentration in supernatant was the result of adsorption, desorption and degradation. But the change of MB concentration in supernatant was mainly determined by adsorption and desorption because the degradation rate of MB was low. During the 12 h long MB degradation reaction, adsorption dominated and the content of MB in supernatant quickly decreased during the first 30 min because of the formation of a large amount of surface peroxide species, and then MB was desorbed from nanoceria in the next 11.5 h due to the decomposition of surface peroxide species with long contact time. That was in accord with the remaining H_2O_2 concentration in system. The 240–290 nm spectral range, which corresponds to the H_2O_2 concentration, showed a continual decrease in absorbance with increasing reaction time (Fig. 6a).

The slow oxidative process of MB was likely due to their stability and difficult degradation. Meanwhile, few surface peroxide species on nanorods, which was caused by the high decomposition activity for H_2O_2, was also one important reason. To further confirm this assumption, we repeated this experiment and added H_2O_2 into

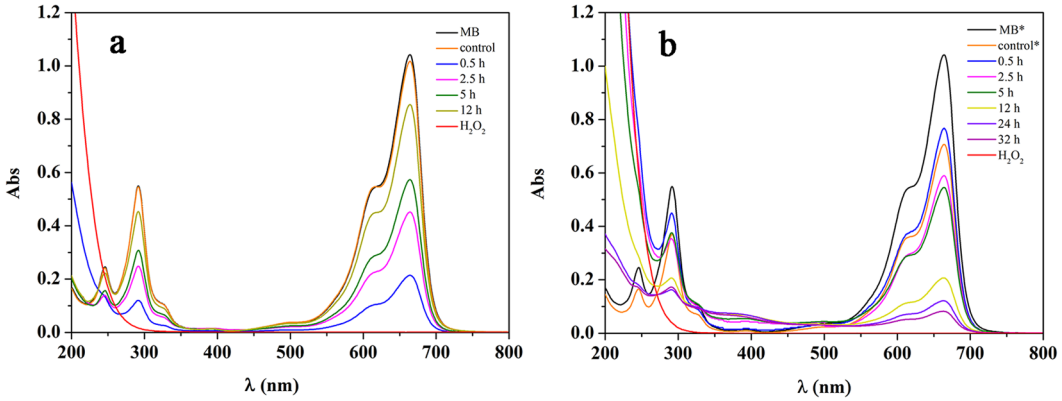

Figure 6. Effect of contact time on MB decolorization in nanoceria/H_2O_2 system (15 mg L^{-1} MB, 1.0 g L^{-1} CeO_2, 20 mM H_2O_2). (**a**) CeO_2 nanorods/H_2O_2 system (The samples were diluted 1:2 in pH 9.0 aqueous solution before tested). (**b**) CeO_2 nanocubes/H_2O_2 system (the samples marked * were diluted 1:2 in pH 9.0 aqueous solution before tested).

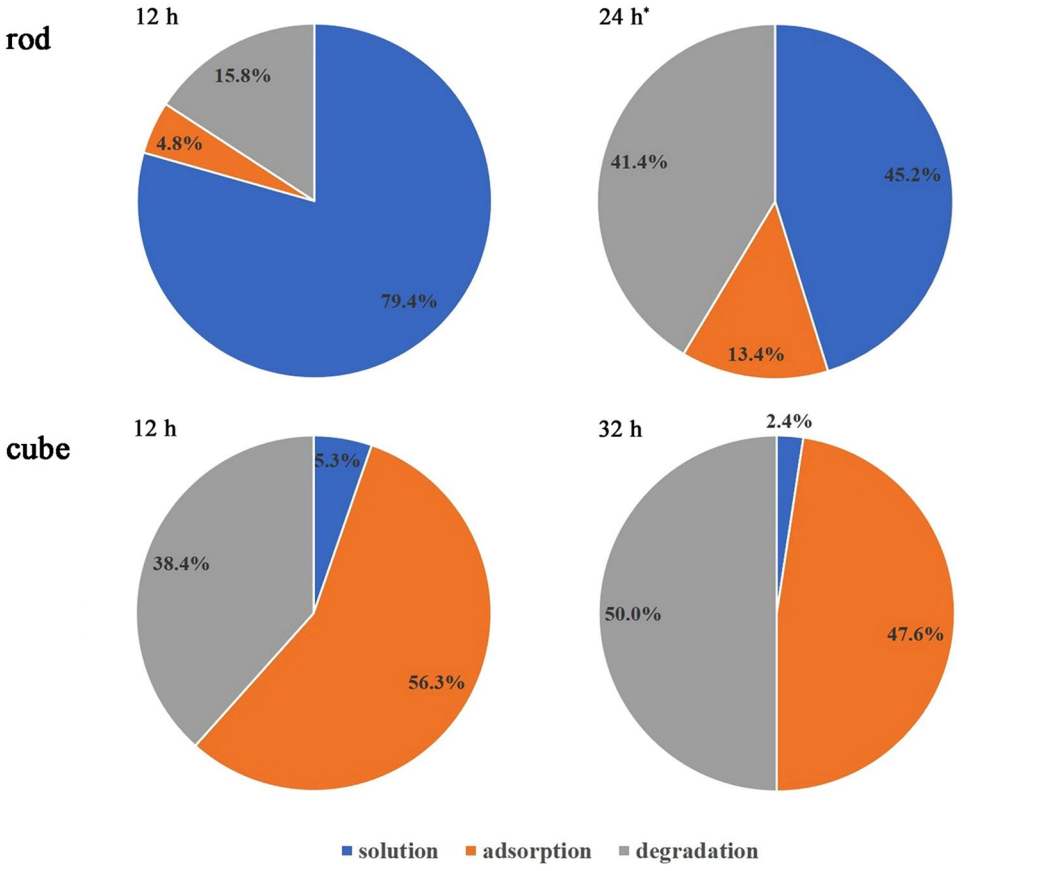

Figure 7. Distribution of MB in nanoceria/H_2O_2 system (*: the addition of H_2O_2 was repeated at 12 h).

the system again at 12 h (the final H_2O_2 concentration at 12 h was still 20 mM). As expected, the proportion of degraded and adsorbed MB increased to 41.4% and 13.4%, respectively (Fig. 7).

However, a different phenomenon was observed in nanocubes/H_2O_2 system. The absorbance band at 664 nm decreased promptly upon the addition of H_2O_2, after which it continued to decrease gradually over the next 32 h (Fig. 6b). The distribution of MB in suspension at 12 and 32 h were shown in Fig. 7. The proportion of degraded MB increased from 38.4% to 50.0%, whereas that of the adsorbed MB decreased from 56.3% to 47.6%, respectively. It could be observed that a small amount of MB dissolved in solution. Thus, the change of MB concentration in supernatant was the result of adsorption and degradation. This can be explained because the catalytic activity of nanocubes towards H_2O_2 decomposition was lower than that of nanorods, and a large number of H_2O_2

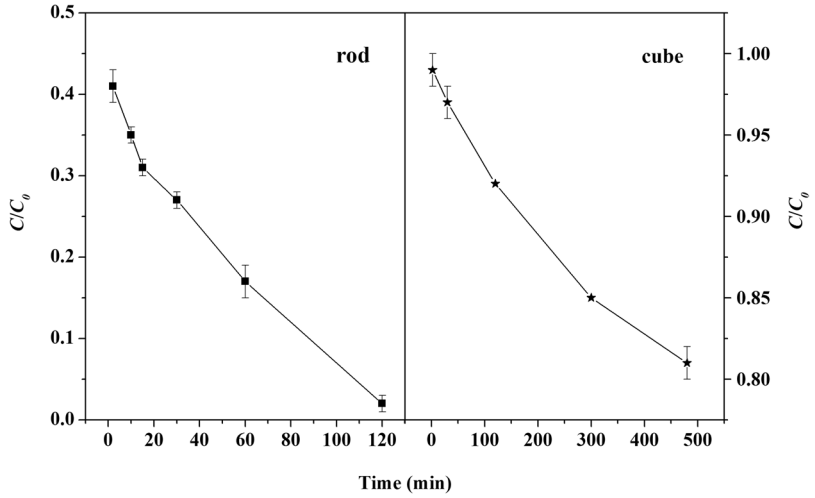

Figure 8. Remove of CR in nanoceria/H_2O_2 system (70 mg L^{-1} CR, 1.0 g L^{-1} CeO_2, 20 mM H_2O_2).

remained in the system (Fig. 6b). The high concentration of H_2O_2 in suspension could continuously provide the surface peroxide species, which caused the adsorption and degradation of MB over nanocubes.

The results suggested that the adsorption and degradation of MB was tightly related to the content of surface peroxide species via Ce^{3+}-H_2O_2 interaction. A high concentration of H_2O_2 in the solution would enhance the adsorption and degradation of MB over the nanoceria surface. But the desorption of MB became dominant after the concentration of H_2O_2 was dramatically decreased.

CR decolorization in nanoceria/H_2O_2 system. The decolorization process of CR in nanoceria/H_2O_2 system was also investigated at 25 °C. Control experiments showed that CR solution was stable in the presence of H_2O_2. The UV−vis spectral changes of the supernatant as a function of time were shown in Fig. S8. In presence of CeO_2 nanorods, the intensity of the characteristic band of CR centered at 497 nm significantly decreased because a lot of CR adsorbed on the surface of nanorods. After the addition of H_2O_2, a quick and obvious increase ($0 < t < 2$ min) of the intensity of the characteristic band of CR was evident at the beginning of degradation. This feature was also observed for CeO_2 nanocubes (Fig. S4b and S8). As previously reported, these features are mostly assigned to the desorption of CR from the surface of CeO_2 because of the adsorption competition between CR and H_2O_2[10,13].

Figure 8 presents the degradation kinetics of CR in nanoceria/H_2O_2 system. Obviously, CeO_2 nanorods exhibited much higher catalytic activity for the degradation of CR than that of CeO_2 nanocubes. 98% degradation of CR was achieved after 2 h of reaction time in nanorods/H_2O_2 system, while the degradation of CR was low, 8% after 2 h and 20% after 8 h, in nanocubes/H_2O_2 system (Figs S4c and S8). The high catalytic activity of the nanorods could be owing to its better redox properties and high concentration of Ce^{3+} [5,6,11,46]. Furthermore, the higher adsorption capability of CR and the larger specific surface area was also conducive to CR degradation[40]. To further verify the importance of adsorption, a control experiment was tested. CeO_2 nanorods was firstly mixed with 20 mM H_2O_2, and CR was added after several minutes. The degradation of CR was significantly decreased to 25.3%. This could be explained by the adsorption competition between CR and H_2O_2.

Reusability of CeO_2 nanorods. The recyclability of CeO_2 nanorods was evaluated by CR degradation at the conditions of pH 9.0, 70 mg L^{-1} of CR, 20 mM of H_2O_2 and 1.0 g L^{-1} of CeO_2. As seen in Fig. S9, the degradation percentage of CR almost kept unchanged during five successive runs after 2 h of reaction, indicating a good reusability of CeO_2 nanorods.

Reaction mechanism discussion. In the nanoceria/H_2O_2 system, the nature of the oxidative species plays a key role in oxidative degradation of organic compounds. According to the literature[8–10,47,48], Ce^{3+} on the surface of nanoceria could complex with H_2O_2 and generate surface peroxide species[13], which would decompose into hydroxyl radicals at low pH or directly act as an oxidative species under alkaline conditions. We speculated that the surface peroxide species should also be the main oxidative species in the current nanoceria/H_2O_2 system because the experiments were performed at pH of 9.0. Based on the experimental observations, the adsorption-degradation processes of MB and CR are schematically illustrated in Fig. 9.

When MB was present in nanoceria/H_2O_2 system, MB could be adsorbed on the surface of nanoceria through electrostatic attraction with surface peroxide species, which subsequently act as the catalytic active sites for MB oxidation[47,48]. With respect to CR, the adsorption of CR on the nanoceria surface is through Lewis acid–base interactions, and the adsorption competition exists between CR and H_2O_2[13,14]. The degradation of CR would occur by attack from the adjacent peroxide species, which would induce an intermolecular rearrangement of CR[8,10] or degrade CR through a homolysis of the O-O bond to form HO[5].

Compared with CeO_2 nanocubes, CeO_2 nanorods displayed a higher catalytic activity for the decomposition of H_2O_2 and generated more surface peroxide species under the current conditions. Therefore, efficient

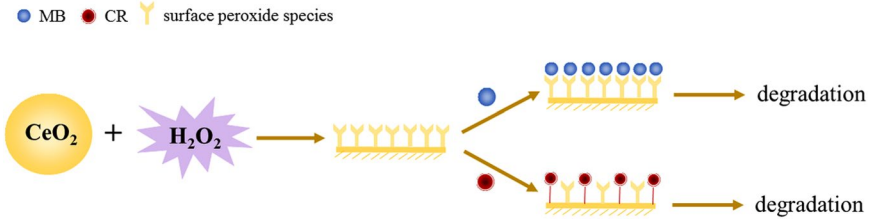

Figure 9. Schematic illustration for the possible mechanism of substrate-dependent Fenton-like activity of nanoceria.

degradation of CR was achieved in CeO_2 nanorods/H_2O_2 system. However, MB could not be efficiently degraded by CeO_2 nanorods in the presence of H_2O_2. The different chemical structure of the organic dyes may be one reason for the difference in the level of degradation because the degradation of MB is generally very difficult[14,49]. Furthermore, the high rate of H_2O_2 decomposition over the ceria nanorods would significantly decrease the concentration of surface peroxide species and the adsorbed MB, and hence the oxidation rate of MB.

Conclusion

The adsorption-degradation of MB and CR in nanoceria/H_2O_2 system was investigated. The MB exhibited weak adsorption over the nanoceria surface via electrostatic attraction, while CR was adsorbed through Lewis acid–base interactions. An adsorption competition existed between CR and H_2O_2, whereas the adsorption of MB was enhanced by the formation of negative surface peroxide species through Ce^{3+}–H_2O_2 interactions. The degradation of CR catalyzed by CeO_2 was much faster than that of MB, and nanorods degraded the CR solution rapidly in comparison to that of nanocubes. In term of different adsorption behavior, two oxidation processes were suggested. MB is adsorbed over the surface of nanoceria through the interaction between MB and surface peroxide species, and the surface peroxide species will act as the catalytic active sites for oxidation of MB. But CR was adsorbed over nanoceria surface and attacked by the adjacent peroxide species, then oxidized into small molecules.

Materials and Methods

Materials. $Ce(NO_3)_3{\cdot}6H_2O$, NaOH, HCl, H_2O_2 (30%, w/w), MB and CR were purchased from Sinopharm Chemical Reagent Co. Ltd (Shanghai, China). All of the reagents were of analytical grade.

Synthesis of CeO_2 nanorods and CeO_2 nanocubes. Nanoceria was synthesized through a hydrothermal process[30,37]. Typically, 40 mL of aqueous solution containing 0.05 g mL^{-1} $Ce(NO_3)_3{\cdot}6H_2O$ and 0.15 g mL^{-1} NaOH was placed in a 50 mL Teflon-lined stainless-steel autoclave and heated. The CeO_2 nanorods were synthesized by hydrothermal treatment at 120 °C for 12 h, and the CeO_2 nanocubes were produced by hydrothermal treatment at 180 °C for 24 h.

Catalyst characterization. The morphology and size of the nanoceria were determined by a high-resolution transmission electron microscope (HRTEM, JEOL, Japan). The powder X-ray diffraction (XRD) patterns were obtained on a D8 Advance X-ray diffractometer (Bruker, Germany). X-ray photoelectron spectra (XPS) measurements were performed on an ESCALAB 250Xi high-performance electron spectrometer (Thermo Fisher, USA). The Brunauer—Emmett—Teller (BET) surface area was measured by N_2 adsorption-desorption isotherms recorded at 77.3 K (Quantachrome, USA). Raman spectra were recorded on a confocal microscopic Raman spectrometer (Renishaw In-Via, USA) with a 532 nm laser light irradiation from 100 to 1200 cm^{-1} at a duration time of 10 s. Before analysis, the samples with and without H_2O_2 treatment were pressed into slices.

The zeta potential of nanoceria as a function of pH was determined by the nanoparticle size and zeta potential analyzer (Horiba, Japan). The concentration of nanoceria was 20 mg L^{-1} and the pH of nanoceria suspensions were adjusted by 0.1 M HCl or 0.1 M NaOH.

Decomposition of H_2O_2. The decomposition of H_2O_2 was carried out in a conical flask (250 mL) placed in a thermostat oscillator (Sunkun, China) with agitation at 200 rpm and 25 °C. 100 mg of the catalyst was added to 100 mL of 20 mM H_2O_2 solution (pH 9.0) as the beginning of the reaction. To avoid the influence of ions on the nanoceria activity, ultrapure water was used in the test, and the pH of the reaction system was adjusted using 0.1 M NaOH solution. At designated time intervals, a certain amount of suspension was taken out and filtered through a 0.22 μm membrane filter. The concentration of H_2O_2 was measured using an UV–vis spectrophotometer (Beijing Purkinje General, China) at 240 nm.

Adsorption of dye in the absence of H_2O_2. The adsorption of the dye was performed in a 25 mL conical flask. Briefly, 10 mg of CeO_2 powder in 10 mL of dye solution was ultrasonically dispersed and shaken at 25 °C. The pH value of the solution was fixed at 9.0, and the concentration of MB and CR was 15 mg L^{-1} and 70 mg L^{-1}, respectively. After 30 min, the suspension solutions in the conical flasks were rapidly filtered through a 0.22 μm membrane filter, followed by immediate measurement of the dye concentration.

Degradation of dye in nanoceria/H_2O_2 system. Generally, 100 mg of catalyst powder was added to 100 mL of dye solution at 25 °C, then H_2O_2 solution was added to reach a concentration of 20 mM and the concentration of dye in suspension was monitored. The initial concentration of MB and CR was 15 mg L^{-1} and 70 mg L^{-1}, respectively. And the initial pH value of reaction system was 9.0. The concentration of MB and CR was measured using an UV–vis spectrophotometer (Beijing Purkinje General, China) at 664 nm and 497 nm, respectively. The all measurements were conducted in triplicate.

References

1. Bokare, A. D. & Choi, W. Review of iron-free Fenton-like systems for activating H_2O_2 in advanced oxidation processes. *J Hazard Mater.* **275**, 121–135 (2014).
2. Aneggi, E., Cabbai, V., Trovarelli, A. & Goi, D. Potential of Ceria-Based Catalysts for the Oxidation of Landfill Leachate by Heterogeneous Fenton Process. *Int J Photoenergy.* **2012**, 694721 (2012).
3. Gan, G. Q. *et al*. A novel magnetic nanoscaled Fe_3O_4/CeO_2 composite prepared by oxidation-precipitation process and its application for degradation of orange G in aqueous solution as Fenton-like heterogeneous catalyst. *Chemosphere.* **168**, 254–263 (2017).
4. Heckert, E. G., Seal, S. & Self, W. T. Fenton-like reaction catalyzed by the rare earth inner transition metal cerium. *Environ Sci Technol.* **42**(13), 5014–5019 (2008).
5. Zang, C., Zhang, X., Hu, S. & Chen, F. The role of exposed facets in the Fenton-like reactivity of CeO_2 nanocrystal to the Orange II. *Appl Catal B-Environ.* **216**, 106–113 (2017).
6. Xu, L. J. & Wang, J. L. Magnetic Nanoscaled Fe_3O_4/CeO_2 Composite as an Efficient Fenton-Like Heterogeneous Catalyst for Degradation of 4-Chlorophenol. *Environ Sci Technol.* **46**(18), 10145–10153 (2012).
7. Lousada, C. M., Yang, M., Nilsson, K. & Jonsson, M. Catalytic decomposition of hydrogen peroxide on transition metal and lanthanide oxides. *J Mol Catal A-Chem.* **379**, 178–184 (2013).
8. Ji, P. F., Wang, L. Z., Chen, F. & Zhang, J. L. Ce^{3+}-Centric Organic Pollutant Elimination by CeO_2 in the Presence of H_2O_2. *ChemCatChem.* **2**(12), 1552–1554 (2010).
9. Cai, W. D., Chen, F., Shen, X. X., Chen, L. J. & Zhang, J. L. Enhanced catalytic degradation of AO7 in the CeO_2-H_2O_2 system with Fe^{3+} doping. *Appl Catal B-Environ.* **101**(1-2), 160–168 (2010).
10. Chen, F., Shen, X. X., Wang, Y. C. & Zhang, J. L. CeO_2/H_2O_2 system catalytic oxidation mechanism study via a kinetics investigation to the degradation of acid orange 7. *Appl Catal B-Environ.* **121**, 223–229 (2012).
11. Wu, T. S. *et al*. X-ray absorption study of ceria nanorods promoting the disproportionation of hydrogen peroxide. *Chem Commun.* **52**(28), 5003–5006 (2016).
12. Artiglia, L., Agnoli, S., Paganini, M. C., Cattelan, M. & Granozzi, G. TiO_2@CeO_x Core-Shell Nanoparticles as Artificial Enzymes with Peroxidase-Like Activity. *ACS Appl Mater Interfaces.* **6**(22), 20130–20136 (2014).
13. Hamoud, H. I., Azambre, B. & Finqueneisel, G. Reactivity of ceria-zirconia catalysts for the catalytic wet peroxidative oxidation of azo dyes: reactivity and quantification of surface Ce(IV)-peroxo species. *J Chem Technol Biotechnol.* **91**(9), 2462–2473 (2016).
14. Issa Hamoud, H., Finqueneisel, G. & Azambre, B. Removal of binary dyes mixtures with opposite and similar charges by adsorption, coagulation/flocculation and catalytic oxidation in the presence of CeO_2/H_2O_2 Fenton-like system. *J Environ Manage.* **195**, 195–207 (2017).
15. Noroozi, B., Sorial, G. A., Bahrami, H. & Arami, M. Equilibrium and kinetic adsorption study of a cationic dye by a natural adsorbent - Silkworm pupa. *J Hazard Mater.* **139**(1), 167–174 (2007).
16. Yagub, M. T., Sen, T. K., Afroze, S. & Ang, H. M. Dye and its removal from aqueous solution by adsorption: A review. *Adv Colloid Interface Sci.* **209**, 172–184 (2014).
17. Ali, H. Biodegradation of Synthetic Dyes-A Review. *Water Air Soil Poll.* **213**(1-4), 251–273 (2010).
18. Wang, Y. C., Shen, X. X. & Chen, F. Improving the catalytic activity of CeO_2/H_2O_2 system by sulfation pretreatment of CeO_2. *J Mol Catal A-Chem.* **381**, 38–45 (2014).
19. Sen, T. K., Afroze, S. & Ang, H. M. Equilibrium, Kinetics and Mechanism of Removal of Methylene Blue from Aqueous Solution by Adsorption onto Pine Cone Biomass of Pinus radiata. *Water Air Soil Poll.* **218**(1-4), 499–515 (2011).
20. Wu, H. & Wang, S. Impacts of operating parameters on oxidation-reduction potential and pretreatment efficacy in the pretreatment of printing and dyeing wastewater by Fenton process. *J Hazard Mater.* **243**, 86–94 (2012).
21. Zheng, J., Gao, Z., He, H., Yang, S. & Sun, C. Efficient degradation of Acid Orange 7 in aqueous solution by iron ore tailing Fenton-like process. *Chemosphere.* **150**, 40–48 (2016).
22. Lin, K. Y. A. & Lin, J. T. Ferrocene-functionalized graphitic carbon nitride as an enhanced heterogeneous catalyst of Fenton reaction for degradation of Rhodamine B under visible light irradiation. *Chemosphere.* **182**, 54–64 (2017).
23. Wan, Z. & Wang, J. L. Ce-Doped zero-valent iron nanoparticles as a Fenton-like catalyst for degradation of sulfamethazine. *RSC Adv.* **6**, 103523–103531 (2016).
24. Wang, Q., Ma, Y. & Xing, S. Comparative study of Cu-based bimetallic oxides for Fenton-like degradation of organic pollutants. *Chemosphere.* **203**, 450–456 (2018).
25. Jiao, Y. *et al*. Facile hydrothermal synthesis of Fe_3O_4@cellulose aerogel nanocomposite and its application in Fenton-like degradation of Rhodamine B. *Carbohyd Polym.* **189**, 371–378 (2018).
26. Soltani, T., Tayyebi, A. & Lee, B. K. Quick and enhanced degradation of bisphenol A by activation of potassium peroxymonosulfate to SO_4 center dot- with Mn-doped $BiFeO_3$ nanoparticles as a heterogeneous Fenton-like catalyst. *Appl Surf Sci.* **441**, 853–861 (2018).
27. Zhou, R., Shen, N., Zhao, J., Su, Y. & Ren, H. Glutathione-coated Fe_3O_4 nanoparticles with enhanced Fenton-like activity at neutral pH for degrading 2,4-dichlorophenol. *J Mater Chem A.* **6**, 1275–1283 (2018).
28. Lee, H. *et al*. Chloride-enhanced oxidation of organic contaminants by Cu(II)-catalyzed Fenton-like reaction at neutral pH. *J Hazard Mater.* **344**, 1174–1180 (2018).
29. Wu, H., Wang, S., Kong, H., Liu, T. & Xia, M. Performance of combined process of anoxic baffled reactor-biological contact oxidation treating printing and dyeing wastewater. *Bioresource Technol.* **98**(7), 1501–1504 (2007).
30. Yang, Z. *et al*. Single-crystalline ceria nanocubes: size-controlled synthesis, characterization and redox property. *Nanotechnology.* **18**(18), 185606 (2007).
31. Ni, P., Wei, X. S., Guo, J., Ye, X. R. & Yang, S. On the origin of the oxidizing ability of ceria nanoparticles. *RSC Adv.* **5**(118), 97512–97519 (2015).
32. Naganuma, T. Shape design of cerium oxide nanoparticles for enhancement of enzyme mimetic activity in therapeutic applications. *Nano Res.* **10**(1), 199–217 (2017).
33. Deshpande, S., Patil, S., Kuchibhatla, S. & Seal, S. Size dependency variation in lattice parameter and valency states in nanocrystalline cerium oxide. *Appl Phys Lett.* **87**(13), 133113 (2005).
34. Liang, F., Yu, Y., Zhou, W., Xu, X. & Zhu, Z. Highly defective CeO_2 as a promoter for efficient and stable water oxidation. *J Mater Chem A.* **3**, 634–640 (2015).
35. Wang, Y. *et al*. Nanocasted synthesis of mesoporous $LaCoO_3$ perovskite with extremely high surface area and excellent activity in methane combustion. *J Phys Chem C.* **112**, 15293–15298 (2008).

36. Tan, H., Wang, J., Yu, S. & Zhou, K. Support Morphology-Dependent Catalytic Activity of Pd/CeO_2 for Formaldehyde Oxidation. *Environ Sci Technol.* **49**, 8675–8682 (2015).
37. Zhou, K. B., Wang, X., Sun, X. M., Peng, Q. & Li, Y. D. Enhanced catalytic activity of ceria nanorods from well-defined reactive crystal planes. *J Catal.* **229**(1), 206–212 (2005).
38. Wei, X. S., Li, X. F., Feng, Y. Q. & Yang, S. Morphology- and pH-dependent peroxidase mimetic activity of nanoceria. *RSC Adv.* **8**(21), 11764–11770 (2018).
39. Xiao, H. Y., Ai, Z. H. & Zhang, L. Z. Nonaqueous Sol-Gel Synthesized Hierarchical CeO_2 Nanocrystal Microspheres as Novel Adsorbents for Wastewater Treatment. *J Phys Chem C.* **113**(38), 16625–16630 (2009).
40. Ji, P., Zhang, J., Chen, F. & Anpo, M. Study of adsorption and degradation of acid orange 7 on the surface of CeO_2 under visible light irradiation. *Appl Catal B-Environ.* **85**(3-4), 148–154 (2009).
41. Srilakshmi, C. & Saraf, R. Ag-doped hydroxyapatite as efficient adsorbent for removal of Congo red dye from aqueous solution: Synthesis, kinetic and equilibrium adsorption isotherm analysis. *Microporous Mesoporous Mat.* **219**, 134–144 (2016).
42. Hao, S. Y., Hou, J., Aprea, P. & Pepe, F. Mesoporous Ce-Pr-O solid solution with efficient photocatalytic activity under weak daylight irradiation. *Appl Catal B-Environ.* **160**, 566–573 (2014).
43. Scholes, F. H., Hughes, A. E., Hardin, S. G., Lynch, P. & Miller, P. R. Influence of hydrogen peroxide in the preparation of nanocrystalline ceria. *Chem Mat.* **19**(9), 2321–2328 (2007).
44. Guzman, J., Carrettin, S. & Corma, A. Spectroscopic evidence for the supply of reactive oxygen during CO oxidation catalyzed by gold supported on nanocrystalline CeO_2. *J. Am. Chem. Soc.* **127**, 3286–3287 (2005).
45. Karakoti, A., Singh, S., Dowding, J. M., Seal, S. & Self, W. T. Redox-active radical scavenging nanomaterials. *Chem Soc Rev.* **39**(11), 4422–4432 (2010).
46. Liu, X. W., Zhou, K. B., Wang, L., Wang, B. Y. & Li, Y. D. Oxygen Vacancy Clusters Promoting Reducibility and Activity of Ceria Nanorods. *J Am Chem Soc.* **131**(9), 3140–3141 (2009).
47. Tian, Z. M. *et al.* Highly sensitive and robust peroxidase-like activity of porous nanorods of ceria and their application for breast cancer detection. *Biomaterials.* **59**, 116–124 (2015).
48. Zhao, H., Dong, Y. M., Jiang, P. P., Wang, G. L. & Zhang, J. J. Highly Dispersed CeO_2 on TiO_2 Nanotube: A Synergistic Nanocomposite with Superior Peroxidase-Like Activity. *ACS Appl Mater Interfaces.* **7**(12), 6451–6461 (2015).
49. Gogoi, A. & Sarma, K. C. Synthesis of the novel beta-cyclodextrin supported CeO_2 nanoparticles for the catalytic degradation of methylene blue in aqueous suspension. *Mater Chem Phys.* **194**, 327–336 (2017).

Acknowledgements

The authors are grateful for the financial support provided by the National Natural Science Foundation of China (Grant No. 21476251).

Author Contributions

W.X.S. and Y.S. conceived the study, as well as wrote the manuscript. W.X.S. and W.Y. carried out the experiments, W.X.S., F.Y.Q., X.X.M. and L.X.F. analyzed the data. Y. S. reviewed and commented the manuscript.

Additional Information

Supplementary information accompanies this paper at https://doi.org/10.1038/s41598-018-36794-2.

Competing Interests: The authors declare no competing interests.

Publisher's note: Springer Nature remains neutral with regard to jurisdictional claims in published maps and institutional affiliations.